Origin of structure and zero-phonon-line anomalies of *X*V centers in diamond (*X* = Si, Ge, Sn, Pb)

Chen Qiu [1], Hui-Xiong Deng,[2,*] Songyuan Geng,[1] and Su-Huai Wei [1,†]

[1]*Beijing Computational Science Research Center, Beijing 100094, China*

[2]*State Key Laboratory of Superlattices and Microstructures, Institute of Semiconductors, Chinese Academy of Sciences & Center of Materials Science and Optoelectronics Engineering, University of Chinese Academy of Sciences, Beijing 100083, China*

(Received 3 January 2023; revised 7 April 2023; accepted 30 May 2023; published 26 June 2023)

Color centers in diamonds have emerged as a promising candidate for quantum information and quantum computing applications. Compared to the well-known and widely studied nitrogen-vacancy N_C-V_C (NV) color center with C_{3v} symmetry, the group-IV vacancy color centers V_C-*X*-V_C (*X*V, *X* = Si, Ge, Sn, Pb), exhibit structures with the D_{3d} symmetry, which give rise to more stable coherent optical transitions for the zero-phonon line (ZPL) due to its inversion symmetry. Moreover, it is experimentally found that the ZPL peak of *X*V centers increases from Si to Sn to Ge to Pb, i.e., it does not vary monotonically with the atomic numbers. So far, the physical origin of the unusual local structures and the abnormal trend of ZPL of the *X*V centers are not well understood. In this paper, based on density-functional theory calculations and symmetry analysis, we demonstrate that the large size of the *X* atoms plays a dominant role in moving the *X* atoms away from the substitution site to the bond-center site between the two carbon vacancies to form the D_{3d} structure that can effectively reduce the local strain energy. Meanwhile, we find that the abnormal trends of ZPL of the *X*V centers derive from a competition of the $p-p$ coupling and $p-d$ coupling between *X* atoms and the divacancy based on the band-coupling mechanism. Our study, therefore, provides insights into the origin of the abnormal trends of ZPL and the local structure of *X*V centers in diamonds.

DOI: 10.1103/PhysRevB.107.214110

I. INTRODUCTION

Point defect-related color centers in diamonds have attracted enormous interest for their potential applications in quantum technologies, such as quantum computing, quantum sensing, and quantum communication [1–8]. The nitrogen-vacancy (NV) color center in diamonds has been studied most extensively and has shown promising results in various experiments [5,9–11]. However, the NV center suffers from weak coherent optical emission, with only 4% (i.e., Debye-Waller factor equals to 0.04) of the fluorescence branching into the coherent zero-phonon line (ZPL) at room temperature [12], resulting in the optical spectral of NV center susceptible to external noise and instability [13–16]. Recently, in order to obtain more stable color center with highly coherent photon emission, much research has focused on the group-IV vacancy color centers, namely, *X*V (*X* = Si, Ge, Sn, Pb) centers. Compared to the NV center, N_C-V_C, created by substituting the C atom with a nitrogen atom adjacent to a lattice vacancy in diamond, which has a local noncentrosymmetric C_{3v} symmetry [Fig. 1(a)], the *X*V color centers spontaneously form a V_C-*X*-V_C local structure, i.e., the *X* atoms migrate from the substitution site to the middle of the two carbon vacancies along the (111) direction, as shown in Fig. 1(b) [17–21]. Because the *X* atoms are located at the bond center of the two vacancies, it has a local centrosymmetric D_{3d} symmetry. Consequently, because *X*V center has the inversion symmetry, there is no permanent electric dipole moment for the *X*V center, which drastically reduces their response to external electric field [22,23]. Therefore, *X*V centers exhibit negligible spectral diffusion and sharp, nearly lifetime-broadened optical emission, and a stable coherent optical transition with high Debye-Waller factor. Despite these advantages of the *X*V centers over the NV center, the physical origin why the *X*V centers have the D_{3d} symmetry is still unclear.

Another interesting observation for the *X*V center is that experimentally, it is observed that the ZPL peak of *X*V centers does not vary monotonically from SiV, GeV, SnV to PbV centers. For example, the negatively charged SiV [SiV^{1-}] center has a sharp ZPL at 738 nm (1.68 eV) at room temperature [20,24], GeV^{1-} has a ZPL transition at 602 nm (2.06 eV) [19,25], but SnV^{1-} has a ZPL transitions at 620 nm (2.00 eV) and PbV^{1-} has a ZPL transitions at 552 nm (2.25 eV) [18,26,27]. The physical origin of this abnormal trend of ZPL peaks for *X*V centers also needs to be better understood for designing the appropriate color center for the varying needs of special quantum applications.

In this paper, we have studied the local structures and ZPL energies of *X*V (*X* = Si, Ge, Sn, Pb) centers in diamonds. Our results reveal that (i) the distinct local structure between NV and *X*V centers origin from relatively large *X* atomic sizes, which leads to *X* atoms spontaneously leaving the substitution site and forming split-vacancy configurations to release the strain energy and lower the energy of occupied electronic states; (ii) the $p-d$ coupling between d orbitals of *M* atoms (*M* = Ge, Sn, Pb) and carbon dangling bonds creates deeper acceptor levels, and thus the transition-energy levels $\varepsilon(0/-1)$ of *X*V centers are monotonically increasing

*hxdeng@semi.ac.cn
†suhuaiwei@csrc.ac.cn

as d-orbital energies of X atoms increase; (iii) due to the competition mechanism of $p-d$ coupling and $p-p$ coupling between the X atoms and carbon dangling bonds, the ZPL energies of XV^{1-} centers show an abnormal trend that ZPL energy of SnV^{1-} center (2.09 eV) is less than that of GeV^{1-} center (2.12 eV). We, therefore, have unveiled the origins of the distinct local structures between XV centers and the abnormal ZPL energies trend of XV^{1-} centers, and reinforced the comprehension of the fundamental properties in group-IV vacancy color centers.

II. COMPUTATIONAL METHOD AND FORMULATION

Our first-principles calculations were carried out using spin-polarized density functional theory (DFT), as implemented in the VASP package, with the Perdew-Burke-Ernzerhof approximation for the exchange-correlation functional [28,29]. The energy cutoff for expansion of the plane waves within the projector-augmentation wave method [30] sets is 400 eV. A 512-atom supercell, which can yield converged charged density by sampling the Brillouin zone only at the Γ point and the Coulomb interactions effect between the periodic cells can be ignored, is adopted to study the properties of XV (X = Si, Ge, Sn, Pb) centers in diamond [17] (see Supplemental Material [31]). All atomic positions were relaxed until the forces on individual atoms fall below 0.02 eV/Å. The excited states were calculated with the constrained-occupation DFT (CDFT) [17], and the atomic positions were relaxed with the excited electronic state within the CDFT method. To obtain the accuracy of electronic band structures and total energies, the Heyd-Scuseria-Ernzerhof (HSE06) hybrid functional method [32,33] with a mixing parameter of 0.28 is adopted. The HSE06 calculation on the primitive cell with the $11 \times 11 \times 11$ special $k-$point mesh resulted in the lattice constant $a_{\mathrm{HSE}} = 3.563$ Å and the indirect band gap $E_g = 5.44$ eV, which is in good agreement with the experimental values of $a = 3.567$ Å and $E_g = 5.48$ eV [34,35].

The formation energy (ΔH_f) of a defect α with charge state q in supercell is given by [36]

$$\Delta H_f(q,\alpha) = \Delta E(\alpha,q) + \sum_i n_i\mu_i + q\varepsilon_F, \tag{1}$$

where

$$\Delta E(\alpha,q) = E_{\mathrm{tot}}(\alpha,q) - E_{\mathrm{tot}}(\mathrm{host}) + \sum_i n_i E_i + q\varepsilon_{\mathrm{VBM}}(\mathrm{host}), \tag{2}$$

where $E_{\mathrm{tot}}(\mathrm{host})$ and $E_{\mathrm{tot}}(\alpha,q)$ are the total energy of host supercell and supercell containing a defect α with charge state q, respectively. μ_i is the chemical potential of each of components i referenced to elemental stable solid/gas with energy E_i; n_i is the number of atoms removed from the host or embedded into the host in introducing the defect α. q is the number of electrons taken from the host to the reservoirs in forming the defect supercell. The eigenvalues are aligned using the same reference level for different supercells.

The defect transition-energy level of $\varepsilon_\alpha(q/q')$ is defined as the Fermi energy E_F at which the formation energy $\Delta H_f(q,\alpha)$ of defect α in charge state q is equal to that of another charge q' of the same defect, i.e., [36]

$$\varepsilon_\alpha(q/q') = \frac{[\Delta E(\alpha,q) - \Delta E(\alpha,q')]}{(q'-q)}. \tag{3}$$

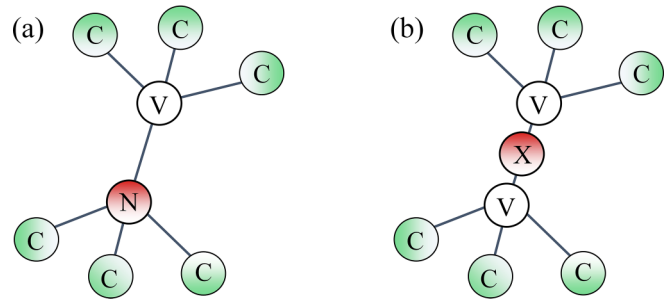

FIG. 1. Schematic plot of local structures of (a) NV center and (b) XV centers. Green balls are carbon atoms, white balls are lattice vacancy, and red balls are impurities.

III. RESULTS AND DISCUSSION

To unveil the physical origin of distinct local structures between XV centers and NV centers in diamonds, we calculated the migration energy barriers of impurity atoms (X, N, C) from substitution site to the middle of the divacancy site along the (111) direction, i.e., from impurity-vacancy configuration [geometry of NV center in Fig. 1(a), denoted as I-V configuration] to vacancy-impurity-vacancy configuration [geometry of XV centers in Fig. 1(b), denoted as V-I-V configuration] with different charged states. It is clearly found that the C-V configuration, i.e., single-vacancy V_C in diamond, has an approximately 2.81-eV migration energy barrier to form a V-C-V configuration with neutral charge state. This is because the formation of V-C-V configuration changes three strong covalent C–C bonds of C-V structure into six relatively weak covalent C–C bonds, and magnifies local structural strain, which largely increases the total energy. To further compare in detail the energy and electronic structure for these two defect configurations, we scrutinize the structural symmetries and the single-particle levels (right panel of Fig. 2). It is found for the CV center that when the structural configuration changes from C-V to V-C-V structure, the corresponding point group reduces from T_d to D_{3d}. In this case, the Γ_5 state located within the band gap splits into a Γ_2^+ state of higher energy and a lower doubly degenerate Γ_3^+ state in the D_{3d} symmetry. The two electrons that originally occupied the Γ_5 state in C-V configuration drop to the Γ_3^+ state in V-C-V configuration, which can lead to 1.14-eV electronic energy gain, as shown in the right panel of Fig. 2(a). Therefore, one can observe that the migration energy barrier between the C-V and V-C-V configurations decreases by 0.6 eV from neutral to negatively charged states (i.e., from $q = 0$ to -1), because more energy gain can be obtained when more electrons occupy the Γ_3^+ state with lower energy. As a result, for the neutral CV center, although the 1.14-eV energy gain derived from occupying lower electronic state favors stabilizing the V-C-V defect configuration, the 3.95-eV energy cost caused by magnifying local structural strain exceeds this energy gain at the V-C-V configuration,

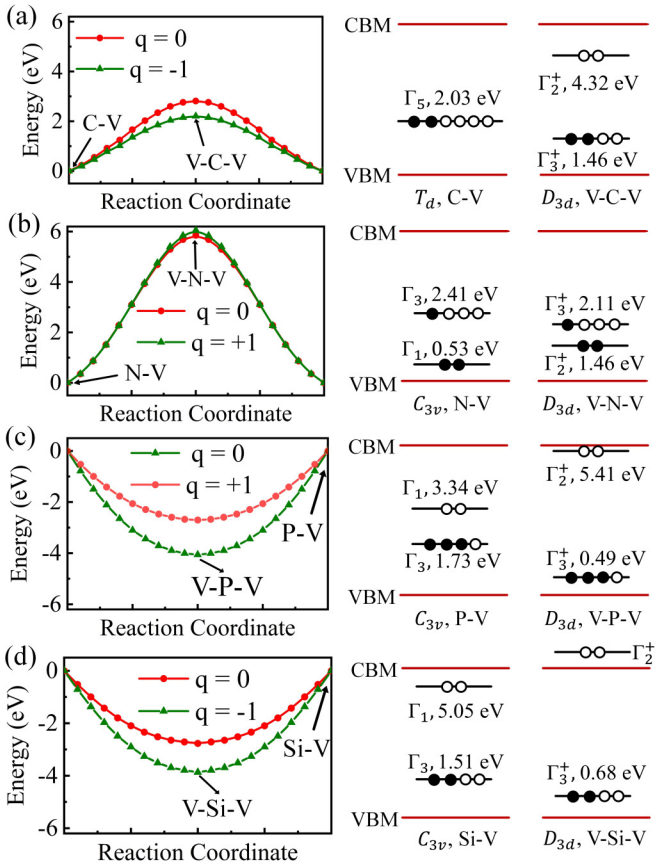

FIG. 2. Left panels of (a)–(d) show HSE-calculated migration energy barriers between impurity-vacancy (I-V) and vacancy-impurity-vacancy (V-I-V) with different charged states (i.e., total energy difference between I-V and V-I-V configuration). Right panels of (a)–(d) indicate HSE-calculated single-particle levels of (a) C-V and V-C-V configurations, (b) N-V and V-N-V configurations, (c) P-V and V-P-V configurations, as well as (d) Si-V and V-Si-V configurations with neutral charge state. All these levels are referenced to the host VBM. Lower and higher red solid line indicates host VBM and conduction-band minimum of diamond, respectively. Solid black balls represent occupation of electrons, and hollow balls indicate occupation of holes. Defect levels' energies, and symmetry are inserted in corresponding positions. Here, we define the sign of migration-energy barrier based on reaction coordinate from I-V to V-I-V configurations.

making it unstable and energetically higher than the stable C-V configuration by 2.81 eV.

When the carbon atom in the C-V center is replaced by a smaller nitrogen atom, the migration energy barrier between the N-V and V-N-V configurations (5.85 eV for neutral state and 6.06 eV for positively charged state) is much higher than that between the C-V and V-C-V configurations due to the large local strain and energy cost due to crystal-field splitting of the electronic structure. Unlike the C-V configuration, the N-V configuration has a reduced C_{3v} local symmetry, whereas V-N-V configuration preserved the D_{3d} point group of V-C-V configuration. Therefore, the Γ_5 state of the C-V configuration within the band gap splits into a lower Γ_1 state and a higher doubly degenerate Γ_3 state in the N-V configuration and the crystal-field splitting decreases from N-V to V-N-V structure because nitrogen is smaller in size and more electronegative than carbon. Thus, from N-V to V-N-V configuration, the energy of the two electrons occupied the Γ_1 state rises 1.86 eV and the energy of the single electron occupied the Γ_3 state drop of 0.3 eV, resulting in 1.56-eV energy penalty of electronic structure. Thus, the migration energy barrier between the N-V and V-N-V configurations also decreases with the increase of defect-state occupations (i.e., from $q = +1$ to 0). Due to the smaller atomic size of N than C atom, from N-V to V-N-V configuration, larger local structural strain and strain energy (4.29 eV) are introduced. These results indicate that both the strain energy cost and electronic energy penalty jointly favor stabilizing the N-V configuration.

However, the carbon atom in the C-V center is replaced by P or Si atom of larger atomic radii, forming the V-P(Si)-V configuration and lowering its energy. Interestingly, contrary to CV and NV centers, the energy lowering between the P(Si)-V and V-P(Si)-V configurations increases with the increase of the defect-level Γ_3^+ occupations (i.e., from $q = +1$ to 0 or from $q = 0$ to -1) in V-P(Si)-V configuration because, due to the crystal-field splitting, the Γ_3^+ level has a lower energy level in V-P(Si)-V configuration than the Γ_3 level in the P(Si)-V configuration. The -3.72-eV (-1.66-eV) energy gain of electronic state is less than the -4.06-eV (-2.77-eV) migration-energy barrier between P(Si)-V and V-P(Si)-V configuration with neutral charge state, which means that the local structural strain is reduced and -0.34 eV (-1.11 eV) strain energy is released from P(Si)-V to V-P(Si)-V structure. The larger strain energy (-1.11 eV) released between Si-V and V-Si-V configuration can be attributed to the larger atomic radius of Si atom compared to P. Indeed, our calculated energy lowering between Ge(Sn, Pb)-V configurations and V-Ge(Sn, Pb)-V configurations increases with the increasing radii of the X atoms and large splitting between the Γ_3^+ and Γ_2^+ states (see Fig. S1 and Table S1 of Supplemental Material [31]). In other words, the synergistic effect of local structural strain relaxation and the occupation of the low Γ_3^+ electronic energy state makes the V-X-V configuration the stable structure, as observed in previous experimental reports [18–21].

Figure 3 shows the HSE-calculated formation energies of XV centers in diamonds as a function of the Fermi level (E_F). It is found that a general trend shows the increasing formation energies with atomic number of the group-IV impurity atoms. This is because a larger atom induces a larger local structural strain, resulting in higher defect-formation energies. These are consistent with the observation that the larger atomic radius for atom X, the longer the C–X bond length between the impurity X atoms and the nearest host C atoms, and the shorter the surrounding host C–C bonds, as shown in Table I. On the other hand, the transition-energy levels $\varepsilon(0/-1)$ of XV centers shift up within band gap with the increasing atomic number of the X atoms [17]. This can be attributed to the emerging $p-d$ coupling and become stronger with the increase in atomic number, which we will further discuss in terms of the band-coupling mechanism.

For the XV centers with V-X-V configurations, the defect states can be considered as a hybridization between the X atoms' orbitals and divacancy states in the host diamond structure. The X atom has six nearest-neighbor C atoms in XV centers, resulting in six C dangling bonds around the X

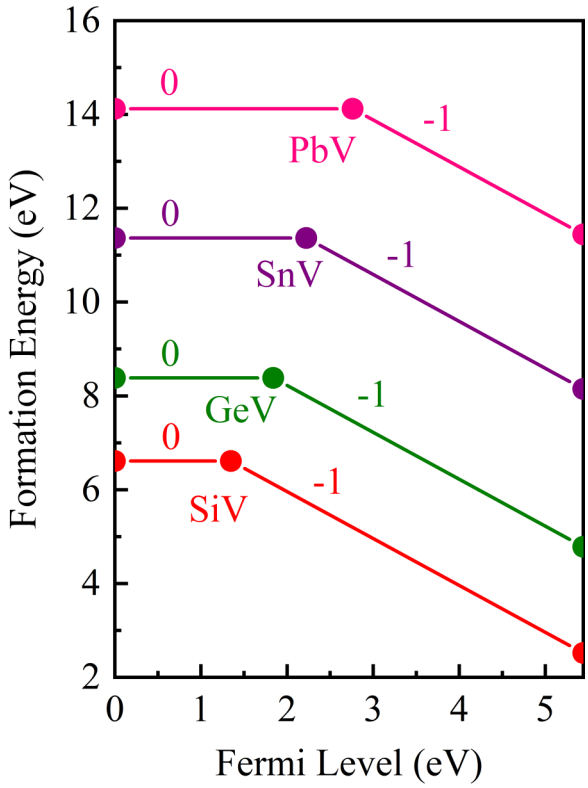

FIG. 3. HSE-calculated formation energies of XV centers in diamond as a function of Fermi level for $q = 0$ and $q = -1$ charge states. Fermi level is referenced to host VBM. We set chemical potential $\mu_i = 0$ for diamond and impurities.

atom. As plotted in Fig. 4, the interactions between the C dangling bonds form a_{1g}, a_{2u}, e_u, and e_g states, and the X atom-related four sp^3 orbitals form a_{1g}, a_{2u}, and e_u states in local D_{3d} crystal field [37]. According to the band-coupling mechanism, from Fig. 4, the a_{1g}, a_{2u}, and e_u states of X atoms and divacancy can couple and form Γ_1^+, Γ_2^-, and Γ_3^- states, as well as Γ_3^+ state, which is almost a pure C dangling-bond orbital in the SiV center. However, the doubly degenerate $d_{xz} + d_{yz}$ and $d_{x^2-y^2} + d_{xy}$ orbitals of M atom (M = Ge, Sn, Pb) have irreducible representation e_g. We find that Γ_3^+ state within band gap is pushed upwards due to the p–d coupling between divacancy and M atom. Indeed, the d-orbital energies increase with the atomic number of M atoms (see Table II), resulting in stronger p–d coupling between divacancy and M atom, thus higher half-occupied Γ_3^+ state energy (see Table S2 and Fig. S2 of Supplemental Material [31]). Therefore,

TABLE I. X-C and C–C bond lengths (in Å) around defect site in fully relaxed systems, compared with C–C bond lengths (1.543 Å) in host.

Systems	X–C bond lengths (Å)	C–C bond lengths around X atoms (Å)
SiV	1.985	1.519 and 1.542
GeV	2.026	1.515 and 1.533
SnV	2.097	1.515 and 1.513
PbV	2.131	1.514 and 1.506

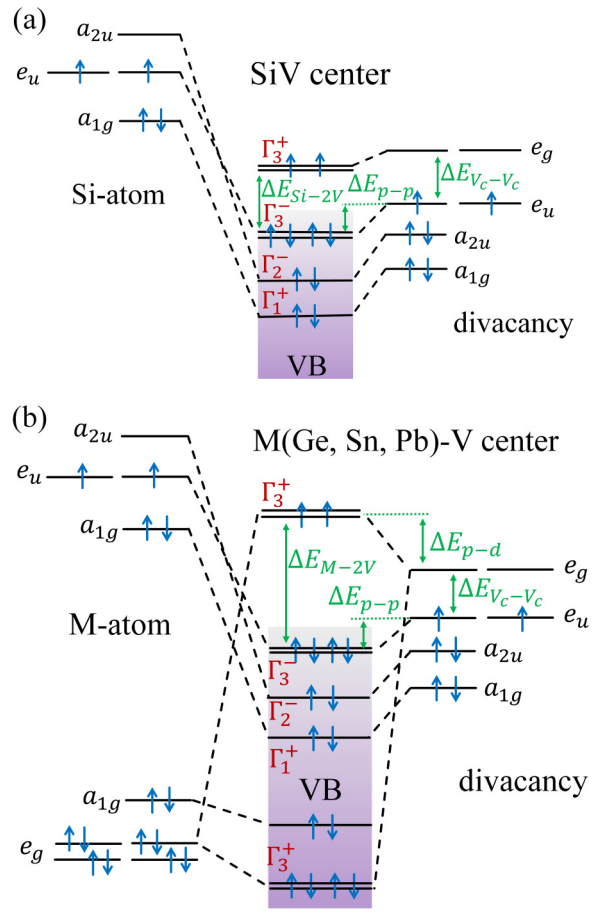

FIG. 4. Band-coupling diagrams of neutral (a) SiV and (b) MV (M= Ge, Sn, Pb) centers in diamond. Irreducible representations of atomic orbitals and band states under D_{3d} point group are shown. Orbitals of (a) Si and (b) M atoms and six-carbon dangling-bond states of divacancy in diamond couples to form the valence band as schematically depicted. For simplicity, level splitting caused by spin-orbital coupling is not considered in diagrams. Coupling strength of SiV^{1-} center and MV^{1-} centers can be described as $\Delta E_{\mathrm{SiV}} = \Delta E_{p\text{-}p} + \Delta E_{\mathrm{Vc-Vc}}$ and $\Delta E_{M\mathrm{V}} = \Delta E_{p\text{-}p} + \Delta E_{\mathrm{Vc-Vc}} + \Delta E_{p\text{-}d}$, respectively. $\Delta E_{p\text{-}p}$ is coupling strength between divacancy and p orbitals of X atoms; $\Delta E_{\mathrm{Vc-Vc}}$ is coupling strength between the divacancy, and $\Delta E_{p\text{-}d}$ is coupling strength between divacancy and d orbitals of M atoms.

when the defect level (half-occupied Γ_3^+ state) of the XV centers traps one electron from valence-band maximum (VBM), it costs more energy with the increased atomic number of X atoms, i.e., an increase of the transition-energy levels $\varepsilon(0/-1)$ of the XV centers.

TABLE II. Atomic orbital-energy levels (in eV) of Si, Ge, Sn, and Pb atoms, respectively.

Atom	Eigenvalue (ns) eV	Eigenvalue (np) eV	Eigenvalue $(n-1)d$ eV
Si	−10.74	−4.01	
Ge	−11.66	−3.82	−29.22
Sn	−10.41	−3.59	−25.77
Pb	−11.87	−3.39	−21.12

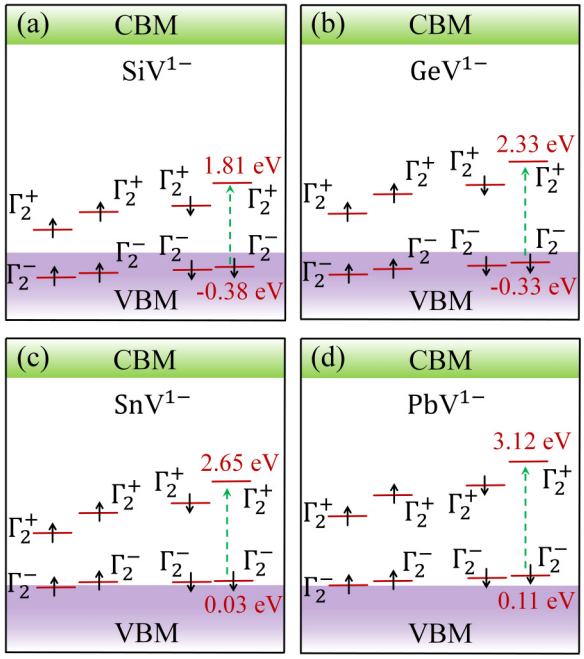

FIG. 5. Defect-level diagrams shows single-particle states for (a) SiV^{1-}, (b) GeV^{1-}, (c) SnV^{1-}, and (d) PbV^{1-} in diamond. Spin-majority and spin-minority channels are denoted by upward- and downward-pointing arrows, respectively. Defect-level energies calculated by HSE06 method, and their symmetry representations are inserted in corresponding positions. All these levels are referenced to host VBM.

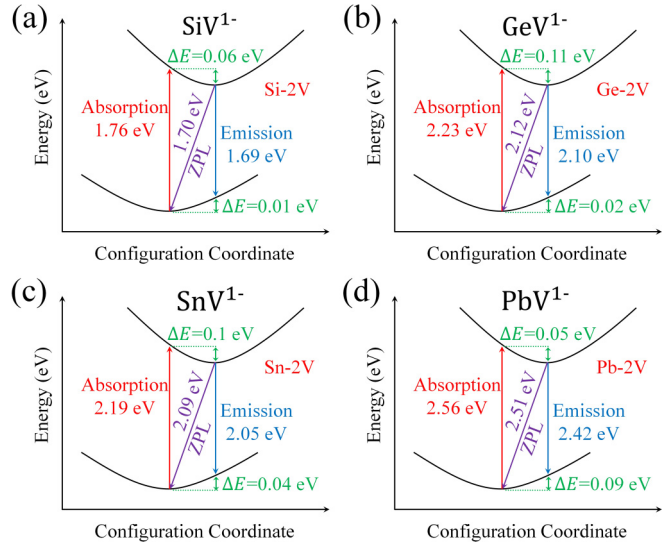

FIG. 6. Configuration coordinate diagrams for spin-conserving triplet excitation. Excitation cycles for (a) SiV^{1-} center, (b) GeV^{1-} center, (c) SnV^{1-} center, and (d) PbV^{1-} center in diamond. Absorption, emission, structure relaxation, and ZPL transitions are indicated, along with their HSE06 calculated energies.

As was reported in the previous studies for the XV center, we find that the local symmetry of XV^{1-} relaxed to lower C_{2h} symmetry from D_{3d} symmetry after HSE06 geometry optimization [17,37]. Consequently, the fourfold degenerate Γ_3^+ state (including spin) within the band gap splits into four Γ_2^+ states, and the Γ_3^- state near valence-band maximum splits into four Γ_2^- states in XV^{1-} structures. As shown by the green dashed arrow in Fig. 5, one can fix the ground-state configuration and excite an electron from the spin-minority channel of the Γ_2^- state into the spin-minority channel of the Γ_2^+ orbital (Fig. 6). The corresponding absorption energies are 1.76, 2.23, 2.19, and 2.56 eV for SiV^{1-}, GeV^{1-}, SnV^{1-}, and PbV^{1-} centers, respectively. Then, one can obtain the ZPL energy after a full relaxation of the crystal configuration while maintaining the excited-state electronic configuration, and the corresponding ZPL energies are 1.70, 2.12, 2.09, and 2.51 eV for SiV^{1-}, GeV^{1-}, SnV^{1-}, and PbV^{1-} centers, respectively, as depicted in Fig. 6. Interestingly, the ZPL energies of XV^{1-} centers are not monotonically increasing but show an abnormal trend between GeV^{1-} center and SnV^{1-} center, i.e., the ZPL energy of SnV^{1-} center (2.09 eV) is less than that of GeV^{1-} center (2.12 eV). It is important to note that the ZPL energy is equal to the absorption energy minus the relaxation energy of excited-state structure. We find that there is only a slight relaxation-energy difference of the excited state between GeV^{1-} and SnV^{1-}, which suggests that the abnormal trend in ZPL energies corresponds to the abnormal trend in absorption energies.

As mentioned above, the half-occupied Γ_3^+ state's energy increase with the increase of d-orbital's energies of M (M= Ge, Sn, Pb) atoms due to stronger p–d coupling of MV^{1-} centers. In addition, the p orbital's energy increases with increasing atomic number of X atoms (see Table II), which raises the energy level of fully occupied Γ_3^- state. As for XV^{1-} centers in Fig. 5, the variation of the Γ_2^- levels is similar to that of the Γ_3^- state since Γ_2^- levels are derived from the Γ_3^- state. The same thing holds for Γ_2^+ levels derived from the Γ_3^+ state. Therefore, the competition mechanism between p–d coupling and p–p coupling jointly determines the energy difference between Γ_2^+ and Γ_2^- states and absorption energies of XV^{1-} centers. Consequently, the ZPL energies of MV^{1-} centers are significantly larger than that of SiV^{1-} centers due to p–d coupling of MV^{1-} centers. The Γ_2^- state shifts up from 0.33 eV below the VBM in GeV^{1-} to 0.03 eV above the VBM in SnV^{1-}, resulting in an upward shift of Γ_2^- state by 0.36 eV. The Γ_2^+ state arises from 2.33 eV above the VBM to 2.65 eV above the VBM in GeV^{1-} and SnV^{1-}, respectively, leading to an upward shift of the Γ_2^+ state's energy by 0.32 eV. Therefore, the Γ_2^- state's energy rise is more than that of the Γ_2^+ state's energy rise, which leads to the absorption energy of SnV^{1-} center being less than that of GeV^{1-} center and is responsible for the abnormal ZPL energies trend between GeV^{1-} center and SnV^{1-} center.

IV. SUMMARY

In summary, we have investigated the properties of group-IV vacancy color centers (XV, X = Si, Ge, Sn, Pb) in diamonds using density-functional theory. Our results demonstrate that the distinct local structure between NV and XV centers is derived from relatively large atomic sizes of the group-IV elements X, which leads to a large local strain energy at the substitutional site and resulting in X atoms spontaneously leaving the substitution site forming split-vacancy local structures with D_{3d} structural symmetry, as

observed in experimental reports. According to this structural symmetry, the shifts up of acceptor transition levels of *X*V centers arise from the stronger $p-d$ coupling between the *M* (*M*= Ge, Sn, Pb) atoms and divacancy, which significantly increase the system energies after defect levels trapping one electron from host VBM. Due to the competition mechanism of $p-d$ coupling and $p-p$ coupling, the absorption energy of exciting one electron from the spin-minority channel of the Γ_2^- state into the spin-minority channel of the Γ_2^+ state in SnV^{1-} center is less than that in GeV^{1-} center; this leads to an abnormal ZPL energy trend of XV^{1-} centers. Our study, thus, provides a more profound and comprehensive insight into the origins of abnormal trends of local structures and ZPL energies in *X*V centers.

ACKNOWLEDGMENTS

This paper was supported by the National Natural Science Foundation of China (Grants No. 11991060, No. 61922077, No. 12088101, No. 61927901, and No. U1930402), the National Key Research and Development Program of China (Grants No. 2020YFB1506400 and No. 2018YFB2200100), the Key Research Program of the Chinese Academy of Sciences (Grant No. XDPB22), and the CAS Project for Young Scientists in Basic Research (Grant No. YSBR-026). We also acknowledge the computational support from the Beijing Computational Science Research Center. H.-X.D. was also supported by the Youth Innovation Promotion Association of Chinese Academy of Sciences under Grant No. Y2021042.

[1] I. Aharonovich, S. Castelletto, D. A. Simpson, C. H. Su, A. D. Greentree, and S. Prawer, Rep. Prog. Phys. **74**, 076501 (2011).
[2] C. E. Dreyer, A. Alkauskas, J. L. Lyons, A. Janotti, and C. G. Van de Walle, Annu. Rev. Mater. Res. **48**, 1 (2018).
[3] J. J. Pla, K. Y. Tan, J. P. Dehollain, W. H. Lim, J. J. Morton, D. N. Jamieson, A. S. Dzurak, and A. Morello, Nature (London) **489**, 541 (2012).
[4] C. Qiu and H.-X. Deng, Sci. China Mater. **65**, 558 (2021).
[5] R. Schirhagl, K. Chang, M. Loretz, and C. L. Degen, Annu. Rev. Phys. Chem. **65**, 83 (2014).
[6] M. E. Turiansky, A. Alkauskas, L. C. Bassett, and C. G. Van de Walle, Phys. Rev. Lett. **123**, 127401 (2019).
[7] J. R. Weber, W. F. Koehl, J. B. Varley, A. Janotti, B. B. Buckley, C. G. Van de Walle, and D. D. Awschalom, Proc. Natl. Acad. Sci. USA **107**, 8513 (2010).
[8] K. Xia, R. Kolesov, Y. Wang, P. Siyushev, R. Reuter, T. Kornher, N. Kukharchyk, A. D. Wieck, B. Villa, S. Yang, and J. Wrachtrup, Phys. Rev. Lett. **115**, 093602 (2015).
[9] A. Dräbenstedt, L. Fleury, C. Tietz, F. Jelezko, S. Killin, A. Nizovtzev, and J. Wrachtrup, Phys. Rev. B **60**, 11503 (1999).
[10] P. J. Vetter, A. Marshall, G. T. Genov, T. F. Weiss, N. Striegler, E. F. Großmann, S. Oviedo-Casado, J. Cerrillo, J. Prior, P. Neumann, and F. Jelezko, Phys. Rev. Appl. **17**, 044028 (2022).
[11] T. K. Unden, D. Louzon, M. Zwolak, W. H. Zurek, and F. Jelezko, Phys. Rev. Lett. **123**, 140402 (2019).
[12] S. Pezzagna, D. Rogalla, D. Wildanger, J. Meijer, and A. Zaitsev, New J. Phys. **13**, 035024 (2011).
[13] H. R. Wei and G. L. Long, Sci. Rep. **5**, 12918 (2015).
[14] L.-X. Sheng, C.-K. Chen, M.-Y. Jiang, X. Li, and X.-J. Hu, Chin. Phys. B **29**, 088101 (2020).
[15] C. Bradac, W. Gao, J. Forneris, M. E. Trusheim, and I. Aharonovich, Nat. Commun. **10**, 5625 (2019).
[16] A. Faraon, C. Santori, Z. Huang, V. M. Acosta, and R. G. Beausoleil, Phys. Rev. Lett. **109**, 033604 (2012).
[17] G. Thiering and A. Gali, Phys. Rev. X **8**, 021063 (2018).
[18] T. Iwasaki, Y. Miyamoto, T. Taniguchi, P. Siyushev, M. H. Metsch, F. Jelezko, and M. Hatano, Phys. Rev. Lett. **119**, 253601 (2017).
[19] M. K. Bhaskar, D. D. Sukachev, A. Sipahigil, R. E. Evans, M. J. Burek, C. T. Nguyen, L. J. Rogers, P. Siyushev, M. H. Metsch, H. Park, F. Jelezko, M. Loncar, and M. D. Lukin, Phys. Rev. Lett. **118**, 223603 (2017).
[20] E. Neu, D. Steinmetz, J. Riedrich-Möller, S. Gsell, M. Fischer, M. Schreck, and C. Becher, New J. Phys. **13**, 025012 (2011).
[21] M. E. Trusheim, N. H. Wan, K. C. Chen, C. J. Ciccarino, J. Flick, R. Sundararaman, G. Malladi, E. Bersin, M. Walsh, B. Lienhard, H. Bakhru, P. Narang, and D. Englund, Phys. Rev. B **99**, 075430 (2019).
[22] R. E. Evans, A. Sipahigil, D. D. Sukachev, A. S. Zibrov, and M. D. Lukin, Phys. Rev. Appl. **5**, 044010 (2016).
[23] C. Hepp, T. Muller, V. Waselowski, J. N. Becker, B. Pingault, H. Sternschulte, D. Steinmuller-Nethl, A. Gali, J. R. Maze, M. Atature, and C. Becher, Phys. Rev. Lett. **112**, 036405 (2014).
[24] J. P. Goss, R. Jones, S. J. Breuer, P. R. Briddon, and S. Öberg, Phys. Rev. Lett. **77**, 3041 (1996).
[25] Y. Zhou, Z. Mu, G. Adamo, S. Bauerdick, A. Rudzinski, I. Aharonovich, and W.-b. Gao, New J. Phys. **20**, 125004 (2018).
[26] S. D. Tchernij, T. Herzig, J. Forneris, J. Küpper, S. Pezzagna, P. Traina, E. Moreva, I. P. Degiovanni, G. Brida, N. Skukan, M. Genovese, M. Jakšić, J. Meijer, and P. Olivero, ACS Photonics **4**, 2580 (2017).
[27] S. Ditalia Tchernij, T. Lühmann, T. Herzig, J. Küpper, A. Damin, S. Santonocito, M. Signorile, P. Traina, E. Moreva, F. Celegato, S. Pezzagna, I. P. Degiovanni, P. Olivero, M. Jakšić, J. Meijer, P. M. Genovese, and J. Forneris, ACS Photonics **5**, 4864 (2018).
[28] G. Kresse and J. Furthmüller, Phys. Rev. B **54**, 11169 (1996).
[29] J. P. Perdew, K. Burke, and M. Ernzerhof, Phys. Rev. Lett. **77**, 3865 (1996).
[30] P. E. Blochl, Phys. Rev. B **50**, 17953 (1994).
[31] See Supplemental Material at http://link.aps.org/supplemental/10.1103/PhysRevB.107.214110 for details on the convergence test of formation energy of SiV center, migration barrier of *M*V centers, calculated single-particle level and $\varepsilon(0/-1)$ defect transition level of *X*V center, and crystal-field splitting of D_{3d} and C_{2h}.
[32] J. Heyd, G. E. Scuseria, and M. Ernzerhof, J. Chem. Phys. **118**, 8207 (2003).

[33] A. V. Krukau, O. A. Vydrov, A. F. Izmaylov, and G. E. Scuseria, J. Chem. Phys. **125**, 224106 (2006).
[34] S. Shikata, T. Tanno, T. Teraji, H. Kanda, T. Yamada, and J.-i. Kushibiki, Jpn. J. Appl. Phys. **57**, 111301 (2018).
[35] M. Cardona and M. L. W. Thewalt, Rev. Mod. Phys. **77**, 1173 (2005).
[36] S.-H. Wei, Comput. Mater. Sci. **30**, 337 (2004).
[37] A. Gali and J. R. Maze, Phys. Rev. B **88**, 235205 (2013).